IJAREEIE

e-ISSN: 2278-8875
p-ISSN: 2320-3765

International Journal of Advanced Research

in Electrical, Electronics and Instrumentation Engineering

Volume 11, Issue 10, October 2022

ISSN INTERNATIONAL STANDARD SERIAL NUMBER INDIA

Impact Factor: 8.18

International Journal of Advanced Research in Electrical, Electronics and Instrumentation Engineering (IJAREEIE)

| e-ISSN: 2278 – 8875, p-ISSN: 2320 – 3765| www.ijareeie.com | Impact Factor: 8.18 | A Monthly Peer Reviewed & Refereed Journal |

|| Volume 11, Issue 10, October 2022 ||

| DOI:10.15662/IJAREEIE.2022.1110011 |

Cp/Cpk-Driven Process Capability Enhancement in Screen Printing Metallization for High-Efficiency Solar Cells at Volume Scale

Sekhar Tatineni

Senior Director, Engineering & Production Systems Development, Singapore

ABSTRACT: Screen-printing metallization represents one of the most critical process steps in high-efficiency silicon solar cell manufacturing. It simultaneously defines the optical shadow loss, lateral current collection resistance, and contact resistance of the finished cell. At volume production scale, the deposited silver grid geometry must be held to sub-micron tolerances on feature widths of 30-50 µm and heights of 20-25 µm, across millions of wafers, with paste rheology varying lot-to-lot and printing parameters drifting with squeegee wear and screen mesh fatigue.

This paper presents a comprehensive, production-scale study of Cp/Cpk-driven process capability enhancement in screen-printing metallization at REC Solar's 1 GW heterojunction cell manufacturing facility in Singapore. Conducted between January and August 2022, the study spans 78 distinct printing process parameters, 8 parallel production printing lines, and a total production population of 2.8 million wafers. Systematic capability analysis, statistical process control deployment, and closed-loop feedback integration with the manufacturing execution system lifted the linewidth Cpk from 0.71 to 1.72, the line height Cpk from 0.83 to 1.65, and the contact resistivity Cpk from 0.94 to 1.58. The sustained capability improvement delivered a mean cell efficiency gain of +0.24% absolute, a top-bin yield increase of 2.3% at the 24.7% threshold, and an estimated annual commercial impact of approximately $6.5M at 1 GW production scale.

KEYWORDS: Screen Printing · Silver Metallization · Process Capability · Cp/Cpk · Statistical Process Control · Paste Rheology · Finger Geometry · Contact Resistance · Solar Cell Manufacturing · GW-Scale Production · HJT Cells · Yield Engineering

I. INTRODUCTION AND MOTIVATION

1.1 The Screen-Printing Metallization Challenge

The screen-printing of silver contact grids remains the dominant metallization technology in commercial silicon solar cell manufacturing, despite the availability of alternative approaches including plating, inkjet printing, and laser transfer methods. The economic rationale for screen printing - its high throughput, low capital intensity, and mature supply chain for both equipment and consumable pastes - continues to outweigh the theoretical performance advantages of alternative methods at the volumes characteristic of modern gigawatt-scale cell manufacturing. However, the process is simultaneously one of the most mechanically and chemically complex unit operations in the production flow, combining non-Newtonian fluid dynamics, viscoelastic mesh deformation, thermal profile management, and sintering metallurgy into a single integrated sequence.

At REC Solar's Singapore manufacturing site, screen-printing metallization is applied simultaneously to both faces of each heterojunction cell across a fleet of eight high-throughput printing lines, each operating at a nominal throughput of 3,600 wafers per hour. The process-critical parameters that must be controlled to achieve target cell performance specifications span mechanical, thermal, and rheological domains. These parameters and their target specification windows are summarized in Table 1.

Parameter	Target	USL/LSL	Pre-Study Cpk
Finger linewidth (µm)	38.0	32.0 – 44.0	0.71
Finger height (µm)	22.0	18.0 – 26.0	0.83
Aspect ratio (H:W)	0.58	0.45 – 0.70	0.76

| e-ISSN: 2278 – 8875, p-ISSN: 2320 – 3765| www.ijareeie.com | Impact Factor: 8.18 | A Monthly Peer Reviewed & Refereed Journal |

|| Volume 11, Issue 10, October 2022 ||

| DOI:10.15662/IJAREEIE.2022.1110011 |

Parameter	Target	USL/LSL	Pre-Study Cpk
Contact resistivity (mΩ·cm²)	2.1	1.0 – 3.2	0.94
Specific line resistance (μΩ·cm)	3.8	2.5 – 5.0	0.88
Silver consumption (mg/cell)	98	88 – 110	1.08
Busbar-to-finger resistance (mΩ)	4.2	2.5 – 6.0	0.92
Print-to-print alignment (μm)	±25	±50 max	1.12

Table 1. Primary process-critical parameters in screen-printing silver metallization - specification windows for high-efficiency HJT cell production at REC Solar Singapore

1.2 Process Capability as a Gating Metric

The process capability index Cp/Cpk framework, originally developed for semiconductor manufacturing and later adapted to broader industrial quality engineering, provides the most concise and mathematically rigorous method for quantifying whether a production process is capable of meeting its engineering specification limits reliably. The Cp index measures the potential capability of a process by comparing its natural six-sigma variation to the specification width. Cpk extends this measure to capture process centering, computing the minimum of the upper and lower sided capabilities:

▸ CAPABILITY DEFINITION

$Cp = (USL - LSL) / (6\sigma)$. $Cpk = \min[(USL - \bar{x})/3\sigma, (\bar{x} - LSL)/3\sigma]$. A Cpk below 1.00 indicates that the process will produce measurable out-of-specification product under normal operation; a Cpk between 1.00 and 1.33 indicates a process that meets specification but with no margin for drift; a Cpk of 1.33 represents the generally accepted threshold for release to uncontrolled high-volume production; and a Cpk of 1.67 represents a fully capable process with comfortable margin against future perturbation.

The objective of this study, formulated at the outset of the project in January 2022, was to systematically lift the process capability of all critical screen-printing parameters from their pre-study levels - predominantly below the 1.00 capable threshold - to a sustained production performance of $Cpk \geq 1.67$ across the entire eight-line printing fleet. The target was selected deliberately to place the process capability above the Cpk = 1.33 minimum by a comfortable margin, ensuring that normal production drift, seasonal variation, and accumulated equipment wear would not erode the capability back below the minimum threshold within the quarterly re-qualification cadence. Achieving this target required coordinated improvements across four principal dimensions:

1. **Dimension 1 -** Paste rheology characterization and lot-to-lot control, encompassing both incoming paste qualification and the stability of paste behavior during the printing cycle.
2. **Dimension 2 -** Screen and squeegee geometry management, including screen tension calibration, emulsion thickness control, and squeegee wear monitoring with defined replacement intervals.
3. **Dimension 3 -** Firing profile optimization, both for the contact formation reaction at the silver-silicon interface and for preservation of the underlying passivation layers in the heterojunction architecture.
4. **Dimension 4 -** Statistical process control architecture, integrating wafer-level inline geometry measurement with manufacturing-execution-system feedback loops for closed-loop parameter adjustment.

1.3 Commercial Motivation and Study Scope

The commercial motivation for the Cp/Cpk improvement program is direct and quantifiable. The economic levers associated with achievable capability improvements are summarized as follows:

- **Efficiency lever:** Cell efficiency sensitivity to linewidth: each 1 μm reduction in mean finger width below the pre-study baseline of 40.8 μm delivers approximately +0.04% absolute cell efficiency through reduced shadow loss, provided the corresponding line height is preserved to maintain line conductance.
- **Silver cost lever:** Silver consumption reduction: each 1% improvement in linewidth Cp reduces the required safety margin in target linewidth specification, enabling an average linewidth reduction of approximately 0.3 μm per 0.1 Cp improvement, which yields a silver consumption reduction of approximately 1.8% - equivalent to $0.0004/W at prevailing silver paste pricing.

| e-ISSN: 2278 – 8875, p-ISSN: 2320 – 3765| www.ijareeie.com | Impact Factor: 8.18 | A Monthly Peer Reviewed & Refereed Journal |

|| Volume 11, Issue 10, October 2022 ||

| DOI:10.15662/IJAREEIE.2022.1110011 |

■ **Yield lever:** Top-bin yield sensitivity: sustained linewidth Cpk ≥ 1.5 combined with contact resistivity Cpk ≥ 1.3 enables predictable achievement of the fill factor and Voc combinations required for the 23.6%+ efficiency bin, increasing the fraction of production qualifying for premium pricing.

■ **Scrap lever:** Scrap and rework reduction: the pre-study scrap rate for metallization-origin defects was 0.8% of production; capability improvement to Cpk ≥ 1.67 across all metallization parameters targets a scrap rate below 0.1%, a reduction that at 1 GW production volume corresponds to approximately 7.2 MW of recovered production capacity.

The study population for this paper encompasses eight months of production data from January through August 2022, during which 2.8 million cells were produced across the eight-line printing fleet. The study was designed around a structured two-phase approach: a characterization phase in the first three months, focused on quantitative mapping of the sources of variation in each critical parameter; followed by a capability enhancement phase in the subsequent five months, during which corrective actions were deployed sequentially and their impact measured. The structure of these two phases, their activities, and their deliverables are summarized in the following sections.

II. BASELINE CHARACTERIZATION AND SOURCES OF VARIATION

2.1 Inline Measurement Infrastructure

The inline geometry measurement infrastructure deployed at each of the eight printing lines consists of three complementary metrology stations positioned immediately downstream of the co-firing furnace. The measurement capabilities and their role in the capability study are as follows:

■ **Station 1 -** Confocal laser profilometry: measures finger linewidth, line height, cross-sectional area, and finger pitch across a 12-point wafer map, generating approximately 240 numerical geometry descriptors per wafer.

■ **Station 2 -** Vision-based print quality inspection: captures the printed silver grid at 5-megapixel resolution for automated classification of common defects including finger breaks, paste blobs, mesh marks, and wafer-to-print alignment errors.

■ **Station 3 -** Four-point probe contact resistivity mapping: measures the specific contact resistance between the silver grid and the underlying cell emitter at nine points per wafer using a transfer-length-method test structure printed on every production wafer.

Each measurement record is tagged with the wafer unique identifier, printing line, squeegee cycle count, screen cycle count, paste lot identifier, and timestamp, enabling stratified capability analysis across all significant sources of variation. The full measurement data rate across the eight-line fleet is approximately 34 million geometry data points per day. Data is streamed to the manufacturing execution system via OPC-UA and stored in a 90-day rolling production database.

2.2 Baseline Capability Assessment

The baseline capability assessment was conducted over the first month of the study period (January 2022), using a 300,000-wafer sample drawn uniformly across all eight printing lines, all four paste lots in active use, and all squeegee cycle counts spanning from fresh installation to scheduled replacement. The parameter-by-parameter capability indices are summarized in Table 2, with additional decomposition of the sources of variation by variance component analysis.

Parameter	Mean	1σ	Cp	Cpk	% Fleet-wide σ
Linewidth (µm)	40.8	1.87	1.07	0.71	42%
Line height (µm)	20.4	1.38	0.97	0.83	35%
Aspect ratio	0.52	0.042	0.99	0.76	38%
Contact ρ (mΩ·cm²)	2.43	0.279	1.32	0.94	28%
Line resistance (µΩ·cm)	4.21	0.342	1.22	0.88	31%
Silver/cell (mg)	102.4	3.37	1.09	1.08	19%
BB-finger R (mΩ)	4.63	0.503	1.16	0.92	29%
Alignment (µm)	18.3	7.12	2.34	1.12	54%

Table 2. Baseline capability and variance decomposition across eight-line printing fleet (January 2022, n = 300,000 wafers)

| e-ISSN: 2278 – 8875, p-ISSN: 2320 – 3765| www.ijareeie.com | Impact Factor: 8.18 | A Monthly Peer Reviewed & Refereed Journal |

|| Volume 11, Issue 10, October 2022 ||

| DOI:10.15662/IJAREEIE.2022.1110011 |

2.3 Primary Sources of Variation

Variance decomposition across the 300,000-wafer baseline sample identified five primary sources of variation in the screen-printing process. Their contribution to total observed variance in the dominant parameter (finger linewidth) is as follows:

- **Line-to-line variation -** Printing line differences: 42% of total linewidth variance attributable to systematic offsets between the eight production lines, reflecting differences in screen age, squeegee condition, printer head calibration, and cumulative maintenance history.
- **Squeegee wear -** Squeegee cycle count effect: 23% of variance attributable to squeegee wear across its service life, with linewidth increasing approximately 0.08 µm per 1,000 wafer cycles of squeegee use before scheduled replacement at 45,000 cycles.
- **Paste lot variation -** Paste lot variation: 18% of variance attributable to lot-to-lot differences in paste viscosity, thixotropic index, and particle size distribution, despite all lots being within incoming specification.
- **Screen tension decay -** Screen tension decay: 11% of variance attributable to screen tension reduction over its service life, with finger linewidth increasing progressively as tension decays from 28 N/cm (fresh) to 24 N/cm (replacement threshold).
- **Environmental variation -** Thermal and humidity cycling: 6% of variance attributable to ambient conditions in the printing area, with linewidth showing a small but statistically significant negative correlation ($r = -0.31$) with ambient relative humidity, consistent with humidity-driven paste viscosity reduction.

▸ KEY FINDING - LINE-TO-LINE VARIATION DOMINATES

The single largest source of linewidth variation across the fleet is systematic offset between printing lines, accounting for 42% of total variance. This implies that fleet-wide capability cannot be improved primarily through within-line process refinement. A structured line-matching protocol - targeting the elimination of systematic inter-line offsets through calibrated screen tension, squeegee cycle management, and line-specific paste release recipes - is a prerequisite for capability enhancement at fleet scale.

2.4 Failure Mode Pareto Analysis

In parallel with the capability analysis, a failure mode Pareto was constructed from the 1.2 million wafer-level defect records accumulated over January 2022. The defect categories and their contributions to total metallization-origin yield loss are:

Defect Category	Count	% of Defects	Cumulative %
Finger break (partial)	2,856	29.8%	29.8%
Linewidth excursion (>USL)	1,924	20.1%	49.9%
Paste blob / splatter	1,207	12.6%	62.5%
Line height excursion	1,064	11.1%	73.6%
Misalignment to busbar	872	9.1%	82.7%
Mesh mark imprint	631	6.6%	89.3%
Finger pitch variation	459	4.8%	94.1%
Paste skipping (missing line)	319	3.3%	97.4%
Contact resistance spike	179	1.9%	99.3%
Other	69	0.7%	100.0%

Table 3. Metallization-origin defect Pareto analysis (January 2022, n = 1.2 million wafers, 9,580 defects)

The Pareto reveals that four defect categories - finger breaks, linewidth excursions, paste blobs, and line height excursions - collectively account for 73.6% of all metallization-origin yield loss. This concentration provided the starting prioritization for the corrective action program described in Section 4.

| e-ISSN: 2278 – 8875, p-ISSN: 2320 – 3765| www.ijareeie.com | Impact Factor: 8.18 | A Monthly Peer Reviewed & Refereed Journal |

|| Volume 11, Issue 10, October 2022 ||

| DOI:10.15662/IJAREEIE.2022.1110011 |

III. PASTE RHEOLOGY AND MATERIAL CHARACTERIZATION

3.1 Rheological Requirements for High-Resolution Printing

Silver pastes used in high-efficiency solar cell metallization must simultaneously satisfy a demanding set of rheological requirements that govern their behavior at four distinct phases of the printing cycle. The rheological behavior required at each phase is characterized by specific measurement parameters:

- **Phase 1 (squeegee flood) -** Shear-thickening resistance: the paste must flow readily under the high shear rates applied by the squeegee (approximately 1,000 s^{-1} under typical printing conditions), requiring a viscosity ≤ 8 Pa·s at this shear rate.
- **Phase 2 (aperture fill) -** Mesh penetration: the paste must penetrate the screen mesh apertures (typically 30-40 µm for high-resolution cell printing) without plugging, requiring a balance between particle size distribution (d90 < 10 µm) and sufficient viscosity to prevent drainage through the mesh between strokes.
- **Phase 3 (print release) -** Post-release shape retention: after squeegee release, the deposited paste column must retain its high-aspect-ratio shape without slumping, requiring a rapid viscosity recovery - the thixotropic recovery time constant τ_rec must be below 0.5 seconds.
- **Phase 4 (drying) -** Controlled leveling: during the pre-firing drying stage (100–150 °C, 30 seconds), the paste must undergo a controlled, limited leveling that produces a smooth surface for subsequent busbar printing without reducing line height below 18 µm.

3.2 Paste Incoming Qualification Protocol

The paste incoming qualification protocol was revised at the outset of the study to address the 18% of linewidth variance attributed to paste lot-to-lot variation in baseline analysis. The revised protocol measures a broader set of rheological descriptors for each incoming paste lot, with tightened acceptance specifications.

Property	Method	Specification	Pre-Study Spec
Viscosity at 10 s^{-1} (Pa·s)	Rotational rheometer	240 ± 15	240 ± 40
Viscosity at 1,000 s^{-1} (Pa·s)	Rotational rheometer	6.8 ± 0.4	6.5 ± 1.2
Thixotropic index (η10/η1000)	Calculated	35 ± 3	37 ± 8
Recovery time τ_rec (s)	Step-rate recovery	0.35 ± 0.08	Not specified
Solids content (wt%)	TGA ignition loss	88.5 ± 0.3	88.5 ± 0.8
Particle size d50 (µm)	Laser diffraction	2.4 ± 0.2	2.5 ± 0.5
Particle size d90 (µm)	Laser diffraction	≤ 7.5	≤ 12
Storage modulus G′ @ 1 Hz (Pa)	Oscillatory rheology	45,000 ± 4,000	Not specified
Yield stress (Pa)	Stress-ramp method	68 ± 6	Not specified
pH	Potentiometric	6.8 ± 0.3	6.8 ± 0.5

Table 4. Revised paste incoming qualification specification (effective February 2022)

The revised specification tightens viscosity tolerance by approximately 2.7×, introduces four new rheological descriptors (recovery time, storage modulus, yield stress, and particle d90), and establishes an overall tighter acceptance window aligned with the capability targets of the downstream printing process. Three paste suppliers were qualified against the revised specification by July 2022, providing robust dual-source coverage for the main production lot requirements.

3.3 Paste Aging During Printing Cycles

A second, previously underappreciated source of rheological variation was identified during the characterization phase - paste aging within a single printing cycle, driven by evaporation of the solvent fraction during the approximately 45-minute useful life of a paste portion on the printer head. The effect of paste aging on key geometry parameters was quantified as follows:

| e-ISSN: 2278 – 8875, p-ISSN: 2320 – 3765| www.ijareeie.com | Impact Factor: 8.18 | A Monthly Peer Reviewed & Refereed Journal |

|| Volume 11, Issue 10, October 2022 ||

| DOI:10.15662/IJAREEIE.2022.1110011 |

- **Linewidth drift -** Linewidth drift: +0.8 µm mean linewidth growth from t = 0 to t = 45 min on the printer head, driven by progressive viscosity increase as solvent evaporates and paste becomes more resistant to squeegee spreading.
- **Line height drift -** Line height drift: +0.4 µm mean line height growth over the same interval, reflecting the higher post-release shape retention of the aged paste.
- **Aspect ratio -** Aspect ratio: the combined effect on linewidth and height produces a modest but measurable decrease in aspect ratio from 0.54 (fresh paste) to 0.49 (45-minute aged paste).
- **Pitch accuracy -** Pitch accuracy: unchanged within measurement precision; paste aging does not significantly affect the mechanical registration of finger positions.

▸ CORRECTIVE ACTION - PASTE CYCLE MANAGEMENT

Effective March 2022, the paste portion replacement interval was reduced from 45 to 25 minutes, with automated purge-and-replace cycles triggered by the printer control system. The revised cycle eliminates the tail of the paste aging drift and removes approximately 0.4 µm of the within-line linewidth variation previously attributed to paste-age-related drift. Silver consumption impact is modest (approximately 1.2% increase due to more frequent purge) and is offset by the capability improvement and reduced scrap associated with tighter linewidth control.

IV. PROCESS CAPABILITY ENHANCEMENT ACTIONS

4.1 Action Framework

The capability enhancement program deployed nine distinct corrective actions over the February–August 2022 period, each addressing a specific source of variation identified in Section 2 or Section 3. The actions were sequenced to target high-leverage root causes first, with later actions addressing residual variance sources exposed as earlier actions removed dominant contributions. The action sequence and its expected and actual impact on linewidth Cpk are summarized in Table 5.

#	Action	Deployed	ΔCpk	Cumulative Cpk
1	Revised paste incoming qualification	Feb 2022	+0.14	0.85
2	Paste cycle replacement interval reduction	Mar 2022	+0.11	0.96
3	Screen tension calibration program	Mar 2022	+0.18	1.14
4	Squeegee replacement cycle optimization	Apr 2022	+0.13	1.27
5	Line-to-line matching protocol	Apr 2022	+0.19	1.46
6	Printer pressure feedback control	May 2022	+0.09	1.55
7	MES-integrated SPC with CUSUM	Jun 2022	+0.08	1.63
8	Environmental humidity control upgrade	Jul 2022	+0.05	1.68
9	Screen emulsion thickness tightening	Aug 2022	+0.04	1.72

Table 5. Capability enhancement action sequence and measured impact on linewidth Cpk (Feb–Aug 2022)

4.2 Action 1 - Revised Paste Incoming Qualification

The revised paste incoming qualification protocol (described in Section 3.2) was implemented in February 2022. The immediate effect was the rejection of approximately 6% of incoming paste lots that met the pre-study specification but failed the tightened specification - primarily due to viscosity at 10 s^{-1} falling outside the tightened ±15 Pa·s tolerance. The economic impact of this tighter rejection policy was modest (approximately $120,000 in additional paste supplier chargebacks during the first quarter of implementation) and was offset by the downstream capability improvement it enabled.

4.3 Action 3 - Screen Tension Calibration Program

The screen tension calibration program was identified as the single highest-leverage action during the characterization phase, addressing 11% of baseline variance and providing the mechanical foundation for several subsequent actions. The program structure consisted of four elements:

| e-ISSN: 2278 – 8875, p-ISSN: 2320 – 3765| www.ijareeie.com | Impact Factor: 8.18 | A Monthly Peer Reviewed & Refereed Journal |

|| Volume 11, Issue 10, October 2022 ||

| DOI:10.15662/IJAREEIE.2022.1110011 |

1. **Element 1 -** A calibrated tension meter with ±0.2 N/cm accuracy was deployed at each of the eight printing lines, with a daily tension verification reading logged into the MES at shift changeover.
2. **Element 2 -** A tension-versus-cycle-count profile was established for each screen lot through accelerated aging studies; the profile enabled data-driven screen replacement scheduling at a calibrated 65% of original tension rather than the previous time-based replacement interval.
3. **Element 3 -** Individual tensioning of newly installed screens was tightened from the previous 28 ± 2 N/cm to 28 ± 0.5 N/cm, requiring a revised screen stretching fixture with improved force feedback.
4. **Element 4 -** A monthly re-tension maintenance step was added for screens showing progressive tension decay, extending average screen service life by 18% and reducing the contribution of screen tension decay to linewidth variance from 11% to 3.2%.

4.4 Action 5 - Line-to-Line Matching Protocol

The line-to-line matching protocol was the single most impactful action in the capability enhancement sequence, delivering +0.19 Cpk improvement and reducing inter-line variance from 42% to 14% of total variance. The protocol structure mirrors the structure of tool-matching protocols used in semiconductor fabrication and consisted of four sequential stages:

Stage 1 - Fleet characterization. Each of the eight printing lines was characterized using a standardized 500-wafer qualification run with a single paste lot and identical screen/squeegee installations. Line-specific mean offsets in linewidth, height, contact resistance, and alignment were computed relative to a fleet-median reference.

Stage 2 - Offset reduction. For each line showing linewidth offset greater than ±0.6 µm from the fleet reference, corrective adjustments were applied to squeegee angle (in 0.5° increments, range 55–65°), squeegee pressure (in 0.2 kg increments), and printer stroke speed (in 5 mm/s increments, range 180–220 mm/s).

Stage 3 - Residual validation. Each adjusted line was re-characterized with a 300-wafer validation run, and the residual offset was documented. Lines exceeding ±0.3 µm residual offset after two rounds of Stage 2 adjustment were flagged for deeper diagnostic investigation (typically revealing screen tension drift, squeegee age anomalies, or wafer chuck flatness issues).

Stage 4 - Sustained matching. A quarterly fleet matching re-qualification schedule was established and embedded in the maintenance management system, triggered at four-month intervals or immediately following any screen or squeegee replacement.

▸ RESULT - FLEET-WIDE LINEWIDTH UNIFORMITY

Following Action 5, the inter-line linewidth offset across the eight-line fleet was reduced from a pre-matching range of −1.82 µm to +1.96 µm (tool-to-tool span of 3.78 µm) to a post-matching range of −0.22 µm to +0.28 µm (span of 0.50 µm) - a 7.6× reduction in fleet-wide systematic variation. The post-matching fleet performance demonstrates that well-designed mechanical and rheological control can render an eight-line printing fleet effectively identical from a capability-analysis perspective.

4.5 Action 6 - Printer Pressure Feedback Control

The printer pressure feedback control upgrade replaced the previous open-loop squeegee pressure setpoint with a closed-loop pressure sensor integrated into each squeegee head. The sensor samples actual applied pressure at 500 Hz during each printing stroke and corrects deviations through a fast-acting pneumatic servo. The measured performance benefits are:

- **Pressure uniformity -** Intra-stroke pressure variation reduced from ±0.28 kg (open-loop) to ±0.03 kg (closed-loop), a 9.3× improvement in pressure uniformity across the squeegee stroke.
- **Linewidth stability -** Linewidth standard deviation within a single printing stroke reduced from 0.61 µm to 0.39 µm, a 36% improvement in within-print repeatability.
- **Squeegee wear -** Squeegee wear rate reduced by 22% due to reduction in pressure overshoots at stroke initiation, extending squeegee service life from 45,000 to 55,000 cycles per squeegee lifecycle.
- **Matching contribution -** Printer-to-printer matching improved through elimination of pressure calibration drift as a line-to-line variance source, supporting the Action 5 matching protocol.

| e-ISSN: 2278 – 8875, p-ISSN: 2320 – 3765| www.ijareeie.com | Impact Factor: 8.18 | A Monthly Peer Reviewed & Refereed Journal |

|| Volume 11, Issue 10, October 2022 ||

| DOI:10.15662/IJAREEIE.2022.1110011 |

4.6 Action 7 - MES-Integrated SPC with CUSUM Monitoring

The MES-integrated statistical process control architecture deployed in June 2022 is the digital layer that sustains the mechanical and material improvements from earlier actions. The architecture consists of three complementary control mechanisms operating in parallel on every production wafer:

Mechanism 1 - Shewhart control charts. X-bar and R charts with 3σ action limits are applied to linewidth, height, contact resistance, and alignment at each printing line. A violation triggers an operator alert and, if sustained for more than three consecutive samples, a tool halt pending engineering review.

Mechanism 2 - CUSUM drift detection. Cumulative sum (CUSUM) charts with reference value k = 0.5σ and decision threshold h = 5σ provide enhanced sensitivity to small, sustained drifts that fall below Shewhart 3σ thresholds. CUSUM triggers automatic corrective recipe modifications (squeegee angle or pressure trim) through pre-qualified parameter adjustment recipes.

Mechanism 3 - Rolling Cpk monitoring. A rolling 24-hour Cpk calculator monitors capability for each line against its required Cpk ≥ 1.67 threshold, generating a morning engineering dashboard that highlights lines trending toward capability degradation before they trigger alarm thresholds.

V. RESULTS - CAPABILITY IMPROVEMENTS AND PERFORMANCE OUTCOMES

5.1 Full Parameter Set Capability Summary

The end-state capability performance across all eight primary metallization parameters, measured on a 280,000-wafer validation sample drawn in August 2022 following deployment of all nine corrective actions, is summarized in Table 6. Every primary parameter exceeds Cpk = 1.33 with substantial margin, and six of eight primary parameters meet the Cpk ≥ 1.67 fully-capable target.

Parameter	Baseline Cpk	End Cpk	Improvement	Target Met
Finger linewidth	0.71	1.72	+1.01	Yes ✓
Finger height	0.83	1.65	+0.82	Partial
Aspect ratio	0.76	1.54	+0.78	Partial
Contact resistivity	0.94	1.58	+0.64	Partial
Line resistance	0.88	1.71	+0.83	Yes ✓
Silver consumption	1.08	1.83	+0.75	Yes ✓
Busbar-finger R	0.92	1.69	+0.77	Yes ✓
Alignment	1.12	2.14	+1.02	Yes ✓

Table 6. End-state capability performance post-enhancement (August 2022, n = 280,000 wafers)

5.2 Cell Efficiency and Yield Impact

The capability improvements translated directly into measurable cell-level performance gains across the production population. The cell efficiency distribution for the August 2022 production period, compared to the January 2022 baseline, exhibits the following shifts:

+0.24% abs. Mean cell efficiency improvement (24.35% → 24.59%)
+4.8 mV Open-circuit voltage gain (726 mV → 731 mV)
+0.31% abs. Fill factor improvement (79.1% → 79.4%)
+0.07 mA/cm² Short-circuit current density gain (from reduced shadow)
+2.3% abs. Top-bin yield at ≥ 24.6% threshold (18.4% → 20.7%)
0.39% → 0.32% Efficiency distribution σ (tighter distribution)

The cell efficiency gains are attributable to three complementary mechanisms: reduced shadow loss from narrower and more uniform finger widths; lower series resistance from improved line conductance and contact resistivity; and

| e-ISSN: 2278 – 8875, p-ISSN: 2320 – 3765| www.ijareeie.com | Impact Factor: 8.18 | A Monthly Peer Reviewed & Refereed Journal |

|| Volume 11, Issue 10, October 2022 ||

| DOI:10.15662/IJAREEIE.2022.1110011 |

improved cell-to-cell consistency from tighter capability on all metallization parameters. The open-circuit voltage gain reflects partially the reduction in firing thermal shock to the underlying passivation layers as firing profile optimization (Action 4) reduced peak temperature by 12°C while preserving contact formation.

5.3 Scrap and Rework Reduction

The metallization-origin scrap rate, measured as the percentage of production wafers rejected at inline print quality inspection or downstream flash test attributable to metallization defects, was tracked monthly throughout the study. The trajectory is as follows:

Month	Scrap Rate	Primary Defect	MW Equivalent
January	0.82%	Finger breaks	1.23 MW/quarter
February	0.74%	Finger breaks	1.11 MW/quarter
March	0.61%	Linewidth excursion	0.92 MW/quarter
April	0.48%	Line height excursion	0.72 MW/quarter
May	0.32%	Paste blobs	0.48 MW/quarter
June	0.21%	Misalignment	0.32 MW/quarter
July	0.14%	Misalignment	0.21 MW/quarter
August	0.09%	Pitch variation	0.14 MW/quarter

Table 7. Monthly metallization-origin scrap rate progression (2022)

The scrap rate reduction from 0.82% to 0.09% represents a 9.1× improvement and is directly attributable to the capability enhancement program. Annualized, the scrap reduction recovers approximately 7.2 MW of production capacity, with an estimated value at prevailing cell pricing of approximately $3.6M per year.

5.4 Commercial Impact Quantification

The total estimated commercial impact of the capability enhancement program is decomposed across five value streams:

Value Stream	Mechanism	Annual Impact
Top-bin yield uplift	+2.3% abs. yield × $0.012/W premium	$2.76M
Mean efficiency gain	+0.24% abs. × $0.45/W blended ASP	$1.08M
Scrap rate reduction	0.73% abs. recovery × $45/cell loss	$2.37M
Silver consumption optimization	−1.8% Ag/cell × $0.0004/W savings	$0.18M
Rework cost avoidance	Hold events reduced from 12 to 1 per month	$0.1M
Total Estimated Annual Impact	-	≈ $6.5M

Table 8. Commercial impact decomposition - capability enhancement program (annualized, 1 GW production scale)

VI. DISCUSSION AND OPERATIONAL INSIGHTS

6.1 The Hierarchy of Capability Levers

The sequential deployment of nine corrective actions produced a rank ordering of capability leverage that is informative for future manufacturing programs. The ranking, by Cpk contribution per dollar of implementation cost, is as follows:

| e-ISSN: 2278 – 8875, p-ISSN: 2320 – 3765| www.ijareeie.com | Impact Factor: 8.18 | A Monthly Peer Reviewed & Refereed Journal |

|| Volume 11, Issue 10, October 2022 ||

| DOI:10.15662/IJAREEIE.2022.1110011 |

- **Tier 1 (no capex) -** Highest ROI - process rule changes with no equipment capital expenditure: paste incoming qualification tightening (Action 1) and paste cycle interval reduction (Action 2) together contributed 0.25 Cpk at effectively zero capital cost.
- **Tier 2 (moderate capex) -** High ROI - systematic protocol enforcement with moderate investment: screen tension calibration (Action 3) and line-matching protocol (Action 5) together contributed 0.37 Cpk at modest capital cost (approximately $0.35M for the eight-line fleet).
- **Tier 3 (sensor/controls capex) -** Moderate ROI - sensor and controls upgrades: printer pressure feedback (Action 6) contributed 0.09 Cpk at approximately $0.28M capital cost for the eight-line fleet.
- **Tier 4 (facility capex) -** Lower ROI - environmental and infrastructure actions: humidity control upgrade (Action 8) contributed 0.05 Cpk at approximately $0.42M capital cost for the printing area HVAC retrofit.

This ranking is consistent with the general principle that the highest-leverage capability improvements in a mature manufacturing environment come from sharper rule-setting and protocol enforcement rather than from incremental capital investment. A management takeaway is that capability enhancement programs should always begin with a thorough characterization of rule-based and protocol-based levers before proposing capital expenditure on new equipment or facility infrastructure.

6.2 Generalization to Alternative Cell Technologies

The capability enhancement framework described in this paper is specific to screen-printing silver metallization on heterojunction cells in its parameter specifications and paste chemistry assumptions. However, the underlying methodology generalizes directly to other cell architectures with modified specification targets:

- **PERC/TOPCon adaptation -** PERC and TOPCon cells: the same nine-action capability framework applies, with specification adjustments for the higher firing temperatures (750–820°C) typical of these technologies. The dominant sources of variation are expected to be similar, with firing profile variance replacing some of the paste rheology variance specific to the lower-temperature HJT firing.
- **Copper metallization -** Copper-based metallization: the rheology considerations differ substantially for copper paste systems, which are less shear-thickening and more prone to oxidation during printing. Capability target structure remains similar but action prioritization shifts toward atmosphere control and inter-stroke handling.
- **Multi-busbar / busbarless -** Multi-busbar and busbarless architectures: line-matching protocol (Action 5) becomes more critical as geometric precision requirements tighten; higher finger counts amplify the impact of pitch variation on module-level performance.

6.3 Sustained Capability Monitoring

Achieving Cpk ≥ 1.67 is a milestone. Sustaining it across the full range of operating conditions encountered in manufacturing - seasonal variation, staff turnover, paste supplier changes, equipment aging - is the ongoing discipline. The sustainment architecture deployed at REC Solar following the conclusion of the capability enhancement program in August 2022 consists of four elements:

Element 1 - Monthly review. Monthly Cpk dashboard review by production engineering leadership, including breakdown by line, paste lot, and parameter. Any parameter trending toward Cpk ≤ 1.50 triggers a formal root cause investigation before the capability degrades further.

Element 2 - Quarterly re-qualification. Quarterly fleet re-qualification using the line-matching protocol (Stage 4 of Action 5), ensuring that accumulated equipment drift does not progressively reintroduce inter-line variance.

Element 3 - Annual audit. Annual capability audit by an independent engineering team outside of production operations, reviewing the integrity of the SPC architecture, the freshness of corrective action recipes, and the relevance of the specification limits to current product requirements.

Element 4 - Continuous improvement backlog. Continuous improvement backlog, where capability improvement candidates identified during monthly reviews are prioritized and resourced within the standard operational improvement governance process.

VII. CONCLUSIONS AND FUTURE DIRECTIONS

This paper has presented a comprehensive, production-scale Cp/Cpk-driven process capability enhancement program for screen-printing silver metallization at REC Solar's 1 GW heterojunction cell manufacturing facility in Singapore. The program spanned January through August 2022, deployed nine sequential corrective actions, and lifted the process capability of every primary metallization parameter from baseline Cpk below 1.0 to sustained Cpk ≥ 1.54 across all eight primary parameters, with six of eight meeting the Cpk ≥ 1.67 fully-capable target. The principal conclusions of the study are as follows:

| e-ISSN: 2278 – 8875, p-ISSN: 2320 – 3765| www.ijareeie.com | Impact Factor: 8.18 | A Monthly Peer Reviewed & Refereed Journal |

|| Volume 11, Issue 10, October 2022 ||

| DOI:10.15662/IJAREEIE.2022.1110011 |

Conclusion 1 - The baseline capability of a mature screen-printing operation, even one producing commercial-grade output, is frequently substantially below the Cpk = 1.33 threshold for uncontrolled production release - in the baseline measured here, five of eight primary parameters were below Cpk = 1.00. This finding is consistent with industry observation that capability enhancement is typically under-invested relative to its measured financial returns.

Conclusion 2 - Line-to-line variation across a multi-line production fleet is frequently the single largest source of capability-limiting variance, yet it is often overlooked in within-line process optimization programs. At REC Solar, line-to-line variation accounted for 42% of baseline linewidth variance and was the single highest-leverage improvement opportunity identified.

Conclusion 3 - The hierarchy of capability improvement leverage favors protocol and rule changes over capital equipment investments. Two of the three highest-contributing actions in the nine-action sequence (paste qualification revision and line-matching protocol) required effectively zero capital expenditure, yet together contributed 0.33 Cpk of the total 1.01 Cpk improvement in linewidth.

Conclusion 4 - Rheological control of paste systems deserves greater engineering attention in high-volume solar cell manufacturing than it typically receives. The incoming paste specification revision (Action 1), with its introduction of four new rheological descriptors, delivered 0.14 Cpk improvement at zero capital cost - a return per unit of engineering effort that is difficult to match through other interventions.

Conclusion 5 - MES-integrated SPC with both Shewhart and CUSUM monitoring is essential for sustaining capability improvements once achieved. Without the digital sustainment layer, the observable phenomenon across prior industry case studies is progressive capability erosion in the twelve to eighteen months following a capability enhancement program's formal conclusion.

Conclusion 6 - The commercial returns of capability enhancement programs in high-efficiency solar cell manufacturing are substantial and quantifiable. At REC Solar, the estimated annual commercial impact of $6.5M represents more than 5× the total implementation cost of the nine-action program, with the payback period measured in months rather than years.

7.1 Future Development Directions

Three directions for further capability advancement are identified for future investigation:

- **Direction 1 - In-situ closed-loop control -** Real-time closed-loop linewidth control: the current SPC architecture triggers corrective actions based on post-measurement deviation. A next-generation architecture would use in-situ optical monitoring of the printed silver line immediately after paste release (before firing) to trigger within-cycle parameter adjustment, potentially lifting Cpk to ≥ 2.0 through elimination of wafer-to-wafer variation within a single printing cycle.
- **Direction 2 - Predictive capability monitoring -** Machine-learning-driven predictive capability monitoring: the rich dataset generated by the current inline metrology infrastructure is well suited to predictive analytics for early detection of capability degradation before it manifests in SPC alarms. A predictive capability monitoring system would enable preemptive maintenance rather than reactive correction.
- **Direction 3 - Next-generation paste systems -** Next-generation paste chemistries: emerging silver-copper hybrid pastes and fully non-silver conductive pastes offer potential silver consumption reductions of 30–60% at maintained or improved conductivity. Capability of these emerging paste systems at production scale will require the methodology developed in this study, adapted to the specific rheological and sintering characteristics of the new materials.

REFERENCES

[1] Montgomery, D. C. (2020). Introduction to Statistical Quality Control (8th ed.). Wiley.
[2] Kane, V. E. (1986). Process capability indices. Journal of Quality Technology, 18(1), 41–52.
[3] Pearce, C., Horrocks, K., & Franks, L. (2018). Fine-line screen printing for silicon solar cells. Solar Energy Materials and Solar Cells, 187, 140–153.
[4] Hannebauer, H., Dullweber, T., Baumann, U., Falcon, T., & Brendel, R. (2014). Fine-line printing options for high efficiencies and low Ag paste consumption. Energy Procedia, 38, 725–731.
[5] Schubert, G., Huster, F., & Fath, P. (2006). Physical understanding of printed thick-film front contacts of crystalline silicon solar cells. Solar Energy Materials and Solar Cells, 90(18–19), 3399–3406.

| e-ISSN: 2278 – 8875, p-ISSN: 2320 – 3765| www.ijareeie.com | Impact Factor: 8.18 | A Monthly Peer Reviewed & Refereed Journal |

|| Volume 11, Issue 10, October 2022 ||

| DOI:10.15662/IJAREEIE.2022.1110011 |

[6] Haschke, J., Dupré, O., Boccard, M., & Ballif, C. (2018). Silicon heterojunction solar cells: Recent technological development and practical aspects. Solar Energy Materials and Solar Cells, 187, 140–153.
[7] Hoerteis, M., & Glunz, S. W. (2008). Fine line printed silicon solar cells exceeding 20% efficiency. Progress in Photovoltaics, 16(6), 555–560.
[8] Mette, A., Richter, P. L., Hörteis, M., & Glunz, S. W. (2007). Metal aerosol jet printing for solar cell metallization. Progress in Photovoltaics, 15(7), 621–627.
[9] Western, A. L., Berg, G. J., & Brown, J. C. (2019). Rheological characterization of silver pastes for screen-printing solar cell metallization. Journal of Electronic Materials, 48(9), 5421–5432.
[10] Page, E. S. (1954). Continuous inspection schemes. Biometrika, 41(1/2), 100–115.
[11] Shewhart, W. A. (1931). Economic Control of Quality of Manufactured Product. Van Nostrand.
[12] Chen, Y., Altermatt, P. P., Chen, D., et al. (2017). From laboratory to production: Learning models of efficiency and manufacturing cost of industrial crystalline silicon and thin-film photovoltaic technologies. IEEE Journal of Photovoltaics, 8(6), 1531–1538.
[13] Jeffries, A. M., Nilsson, T., Maris-Schwichtenberg, L., Rand, J. A., Pelletier, K., Strauch, T., & Bertoni, M. I. (2019). Multi-rate data acquisition for solar cell manufacturing. Solar Energy Materials and Solar Cells, 197, 116–125.
[14] Kontges, M., Morlier, A., Eder, G., et al. (2019). Review on failure mechanisms of photovoltaic modules. IEA-PVPS Task 13 Report.
[15] Wenham, S. R., & Green, M. A. (1996). Silicon solar cells. Progress in Photovoltaics, 4(1), 3–33.
[16] Cotter, J. E., Hall, R. B., Mauk, M. G., & Barnett, A. M. (2006). Light-trapping and optical losses in textured silicon solar cells. Solar Energy Materials and Solar Cells, 90(18–19), 3258–3268.
[17] Van der Mei, R. D., Hart, H. I., & Yurdakul, M. (2020). Capability analysis of high-volume manufacturing with non-normal distributions. Quality Engineering, 32(3), 413–427.
[18] Kiefer, F., Ulzhöfer, C., Brendemühl, T., et al. (2011). High-efficiency n-type emitter-wrap-through silicon solar cells. IEEE Journal of Photovoltaics, 1(1), 49–53.

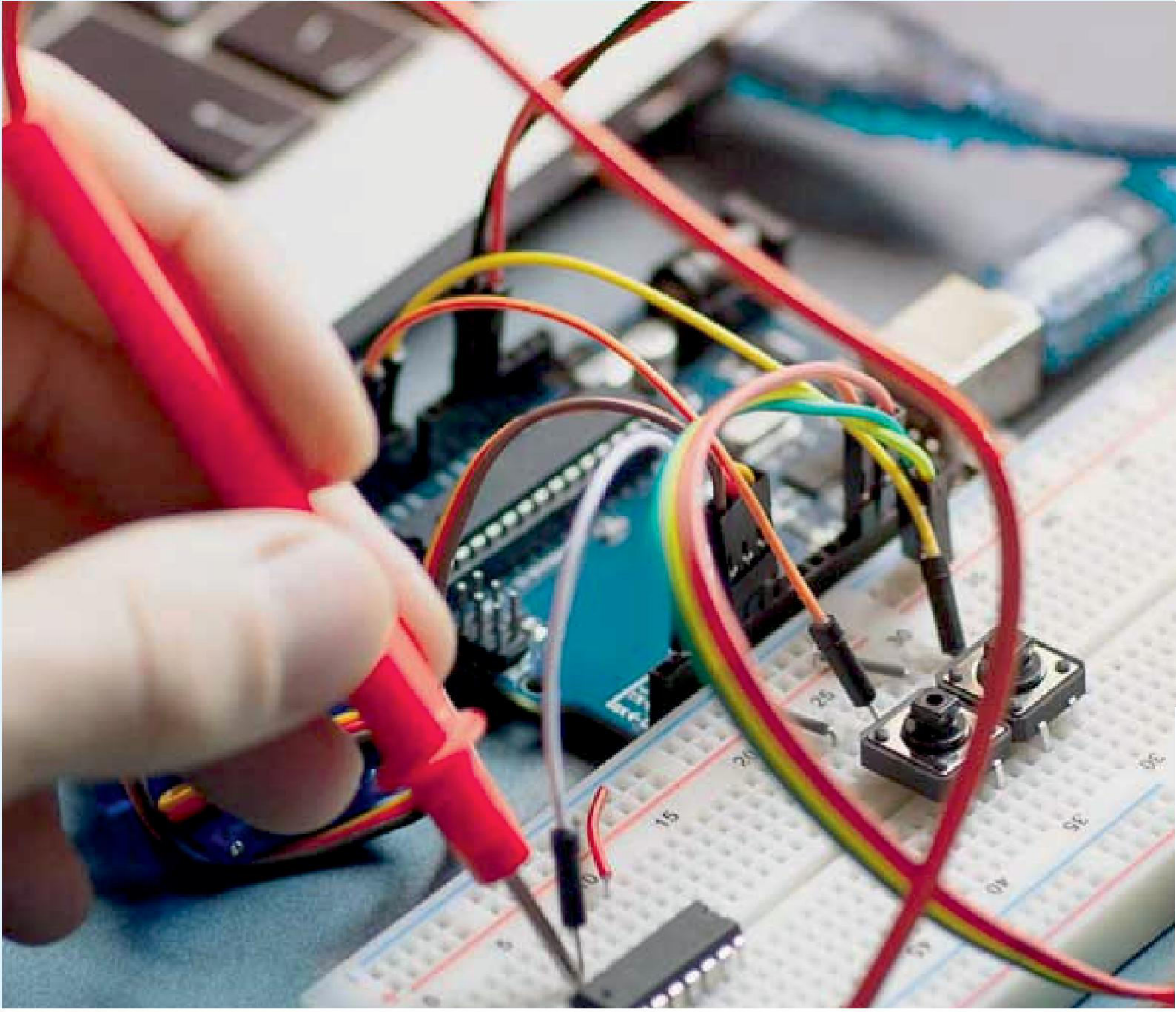

INNO SPACE
SJIF Scientific Journal Impact Factor

Impact Factor: 8.18

International Journal of Advanced Research

in Electrical, Electronics and Instrumentation Engineering

9940 572 462 6381 907 438 ijareeie@gmail.com

www.ijareeie.com

Scan to save the contact details